# Fabrication and Structural Properties of CuO Doped $SnO_2$ Nanostructured Thin Films

Kyaw Kyaw[1], Hnin Yu Khaing[2]

## Abstract

The main objective of this research paper was to study the structural and optical properties of copper oxide (CuO) doped tin oxide ($SnO_2$) nanostructured thin films using sol-gel method. Tin (II) chloride, copper (II) chloride, ethanol and deionized water were used as main precursor solution. Fabricated CuO:$SnO_2$ thin films were characterized with X-ray diffraction (XRD) technique to investigate their structural properties. Scanning electron microscopy (SEM) was used to analyze the surface morphological properties of the obtained thin films. Band gap energies of the fabricated thin films were characterized with UV-Vis Spectroscopy and the product percentage of the sol-gel method was confirmed with EDXRF analysis. The observed XRD profiles showed the tetragonal crystal structure of CuO:$SnO_2$ nanostructured thin films. The average crystallite sizes were 52.035 nm, 26.927 nm, 37.757 nm, 30.874 nm and 17.517 nm. The surface morphological properties of the fabricated thin films were observed from the SEM analysis and it was revealed that the grain size distribution of the films depended on the amount of CuO doping.

## Introduction

Tin oxide ($SnO_2$) is wide band gap n - type semiconductor that exhibits high transparency to visible and near infrared (NIR) regions of electromagnetic spectrum. They are odorless, flammable and have high boiling point (1800-1900ºC). Most of tin oxide materials have rutile (tetragonal structure) phase, and under high pressure and temperature it can be found in orthorhombic structure. Nowadays, $SnO_2$ is widely used in electronics devices, such as light emitting diodes (LEDs), heat mirror, solar cells, solid stage gas sensors and thin film gas sensors, because of its good physical and chemical properties such as high transparency, low cost, high electrical conductivity and low resistance [Sinopoli *et al*]. The $SnO_2$ exhibits good activity and stability under irradiation in both acidic and basic atmosphere. However, the pure $SnO_2$ shows much lower photocatalytic activity even under UV irradiation due to its large band gap (~3.6 eV). To improve its photocatalytic activity, it is necessary to dope with other lower band gap semiconductor materials. The CuO is a p-type semiconductor with a small band gap (~1.7 eV). When $SnO_2$ has doped with the CuO, the n($SnO_2$)/ p(CuO) heterojunctions can be obtained and the photo-generated electrons from $SnO_2$ can easily migrate to CuO. This will help to separate photo-generated electrons with holes, leading to enhance the photocatalytic properties. $SnO_2$ nanoparticles are synthesized by various method such as sol-gel method, hydrothermal method, co-precipitation method, mechanochemical method, spray pyrolysis method and electrochemical deposition method, etc. Sol-gel method is the best method to synthesize $SnO_2$ nanoparticles for controlling the size of the nanoparticles under the atmospheric pressure and low temperature [Galioglu *et al*]. In this research, CuO doped $SnO_2$ nanostructured thin films were prepared by sol – gel method and spin coating method. The structural, morphological and optical properties of fabricated thin films were investigated.

[1] Lecturer, Department of Physics, University of Mandalay
[2] Lecturer, Department of Physics, Yenangyaung Degree College

## Experimental Procedure

### Synthesis of CuO doped $SnO_2$ nanoparticles

In this present work, $SnCl_4$ (Tin tetrachloride), ethanol and deionized water were used as starting materials. Firstly, 20 ml of deionized water were mixed with 10 ml of ethanol and stirred at 600 rpm for 5 min. And then 5 g of $SnCl_4$ was added to the ethanol solution and stirred continuously at 600 rpm for 1 h under aluminum fume hood. After adding $SnCl_4$, the color of solution was immediately turned to brownish yellow color and it could be revealed that $SnO_2$ nanoparticles were formed. (0.02 g, 0.04 g, 0.06 g, 0.08 g and 0.1 g) $CuCl_2$ were added respectively to the solution of $SnCl_4$ and stirred at 600 rpm for 1 h. The obtained solutions were annealed at 300ºC for 2 h to obtained CuO doped $SnO_2$ nanoparticles. The synthesized powders were washed with deionized water and ethanol to remove chemical impurities. The chemical compositions and oxide bonds of the obtained power were investigated with EDXRF analysis.

### Fabrication of $SnO_2$:CuO nanostructured thin films

The obtained 0.25 g of $SnO_2$:CuO powders were mixed with ethanol and acetone solutions by using magnetic stirrer for 5 min to get the uniform gel for spin coating process. The 200 µl of $SnO_2$:CuO precursor solutions were deposited onto the chemically cleaned glass substrates at 5000 rpm for 20 s. The obtained thin films were annealed at 300˚C for 30 min. The structural, morphological and optical properties of fabricated thin films were investigated with XRD, SEM and UV-Vis spectrophotometer. The block diagram for the fabrication of CuO doped $SnO_2$ nanostructured thin films was illustrated in Fig 1.

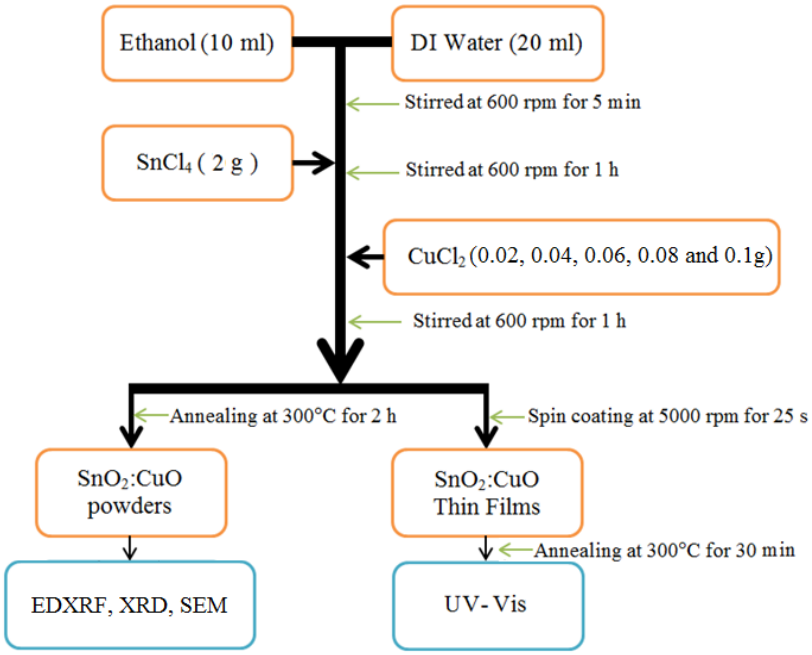


Fig 1. The block diagram for the fabrication of $SnO_2$: CuO nanostructured thin films.

## Results and Discussion

### EDXRF Analysis for Oxide Bond

EDXRF method was used to analyze oxide bonds of the fabricated thin films. Fig 2 showed the amount of count versus energy spectrum of the $SnO_2$:CuO thin film. The amount of oxide chemicals were tabulated in Table 1.

Table 1. The amount of oxide chemicals in $SnO_2$:CuO thin film.

| No | Oxides | Content Amount (%) |
|---|---|---|
| 1 | $SnO_2$ | 98.619% |
| 2 | CuO | 1.244% |
| 3 | PbO | 0.026% |
| 4 | $Fe_2O_3$ | 0.032% |

According to EDXRF analysis, $SnO_2$:CuO nanoparticles were successfully synthesized. $SnO_2$ 98.619% was obtained from the sol-gel method and the amount of sample percentage could be confirmed as pure $SnO_2$ material. The doped CuO percentage was observed as 1.244% at 300℃ for 2 h.

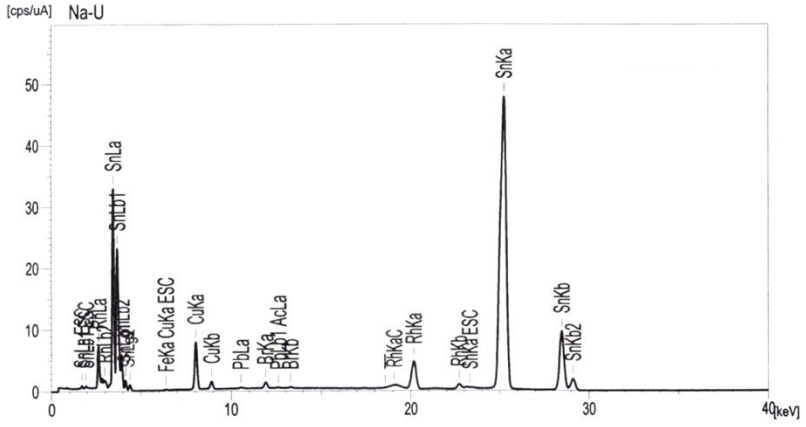


Fig 2. The amount of count versus energy spectrum of the $SnO_2$:CuO thin film.

### Structural Analysis with XRD

The XRD profiles of $SnO_2$:CuO nanostructured thin films were shown in Fig 3(a, b, c, d and e) respectively. The peaks were observed between the 2θ diffraction angle values between 10° and 70°. From these figures, it was observed that the sharp diffraction peaks were observed and it could be noted that the obtained films had crystalline nature. The fabricated thin films were in the tetragonal structure and they were good agreement with standard libraries of $SnO_2$ (JCPDS Card No.41-1445). The (110) peaks had the highest intensities in all XRD profiles but other peaks like (101), (111), (211) and (112) were clearly identified. (110) plane indicated $SnO_2$ nanoparticles and (111) plane represented CuO dopant. These count of dominant peaks were increasing with CuO doping ratios. The crystallite sizes were calculated using Debye-Scherer's formula and their crystallite sizes were tabulated in Table 2.

Table 2. The crystallite sizes of $SnO_2$:CuO thin films from XRD profiles.

| No | CuO (g) | Crystallite Size (nm) |
|---|---|---|
| 1 | 0.02 | 52.035 |
| 2 | 0.04 | 26.927 |
| 3 | 0.06 | 37.757 |
| 4 | 0.08 | 30.874 |
| 5 | 0.1 | 17.517 |

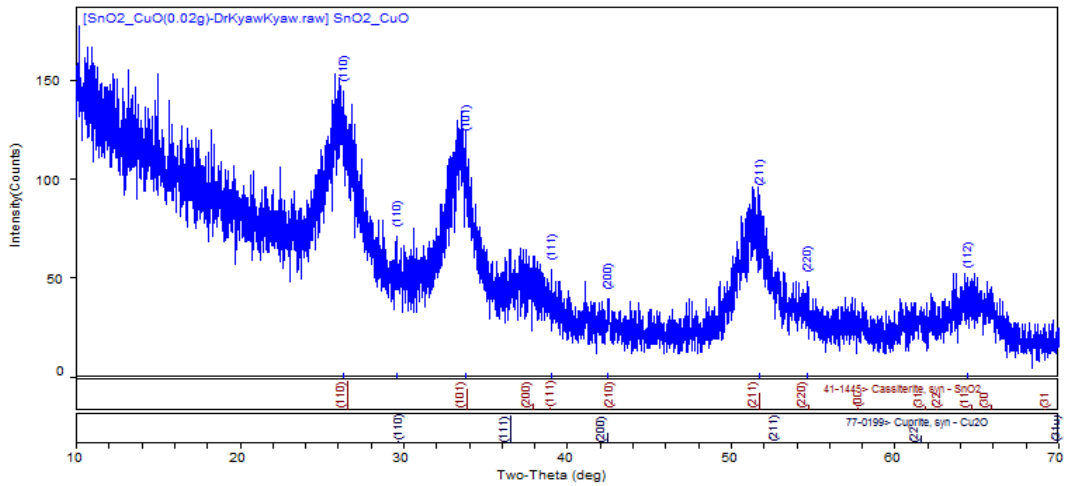


Fig 3(a). XRD profiles of $SnO_2$:CuO (0.02g) thin film.

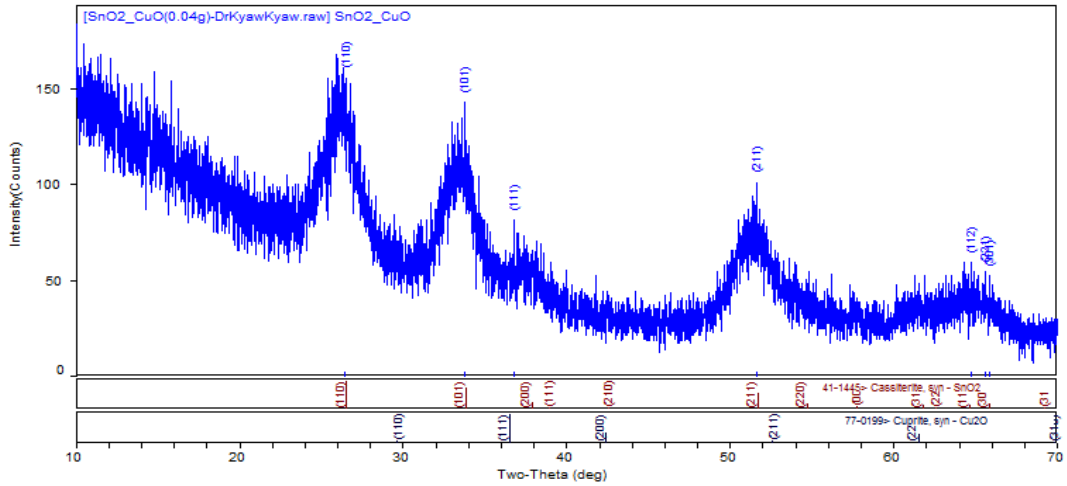


Fig 3(b). XRD profiles of $SnO_2$:CuO (0.04g) thin film.

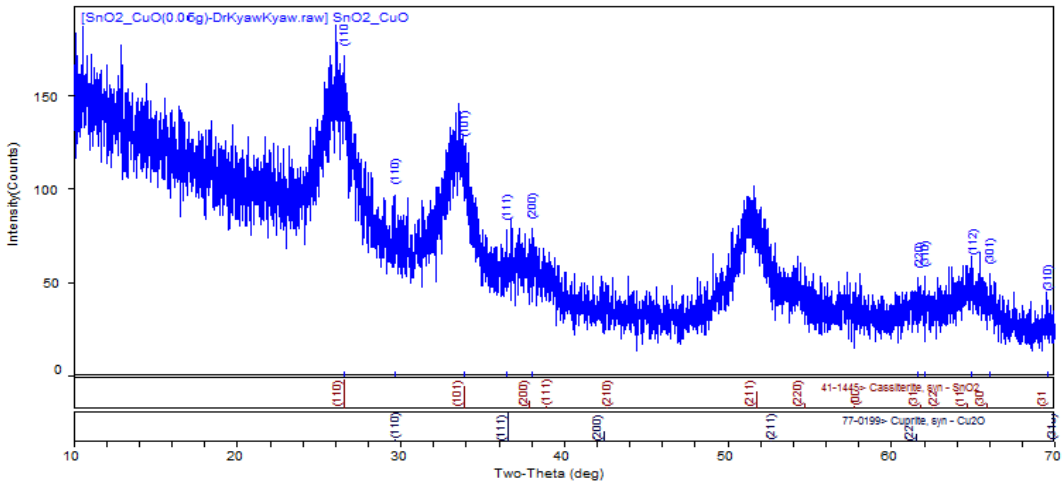


Fig 3(c). XRD profiles of $SnO_2$:CuO (0.06g) thin film.

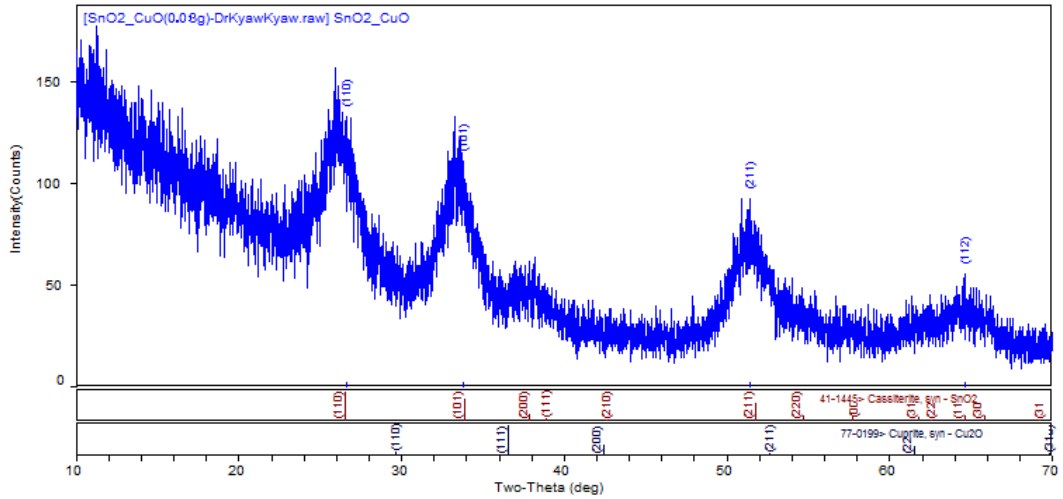


Fig 3(d). XRD profiles of $SnO_2$:CuO (0.08g) thin film.

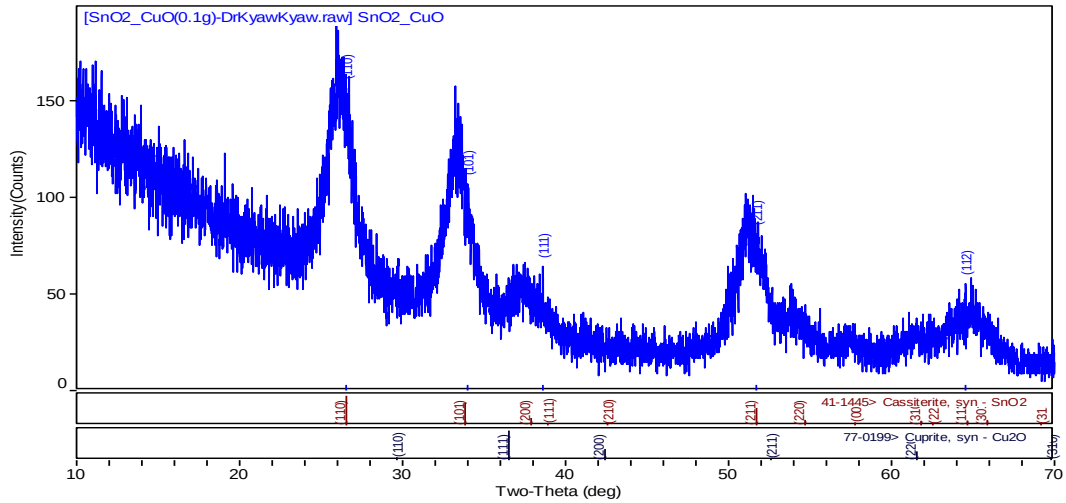


Fig 3(e). XRD profiles of $SnO_2$:CuO (0.1g) thin film.

**Morphological Properties Analysis with SEM**

The surface morphological properties of $SnO_2$:CuO thin films had been carried out by using Scanning Electron Microscope (SEM). Fig 4(a, b, c, d and e) showed the SEM micrographs of $SnO_2$: CuO thin films with different CuO doping ratios. From the Fig 4(a) SEM micrograph of $SnO_2$:CuO (0.02 g), nanoparticles showed irregular shape and agglomerated in micro-scaled particles. In the Fig 4(b) SEM micrograph of $SnO_2$:CuO(0.04 g), it could be found that agglomerated nanoparticles were overlapped in some region. From the Fig 4(c and d) SEM micrographs for CuO (0.06 g and 0.08 g) thin films, nanoparticles were in uniform spherical shape. Some grains were collected in some region due to the increase of CuO doping. It was observed from the Fig 4(e) SEM micrograph of CuO (0.1 g) doped thin film, nanoparticles were formed as clusters and agglomerated in mixed form of micro and nanoparticles. It was noted that the doping amount would increase the agglomeration. The average grain size of $SnO_2$:CuO (0.02, 0.04, 0.06, 0.08 and 0.1 g) were tabulated in Table 3.

Table 3. The average grain sizes of the $SnO_2$:CuO thin Films from SEM Analysis.

| No | CuO (g) | Average Grain Size (nm) |
|---|---|---|
| 1 | 0.02 | 798 |
| 2 | 0.04 | 662 |
| 3 | 0.06 | 412 |
| 4 | 0.08 | 726 |
| 5 | 0.1 | 1120 |

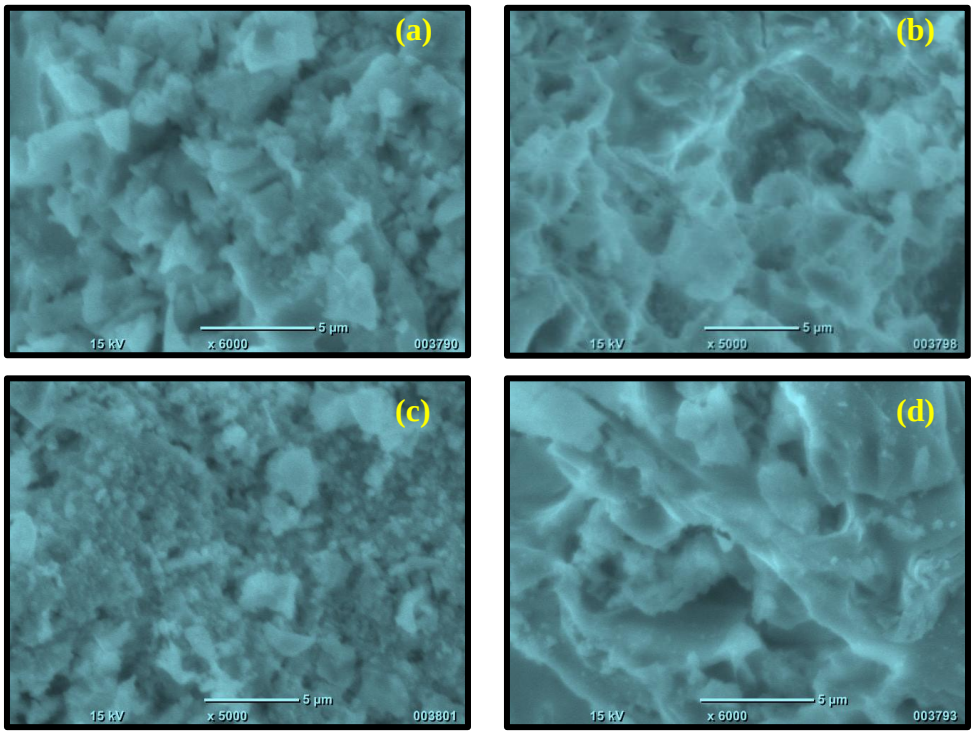

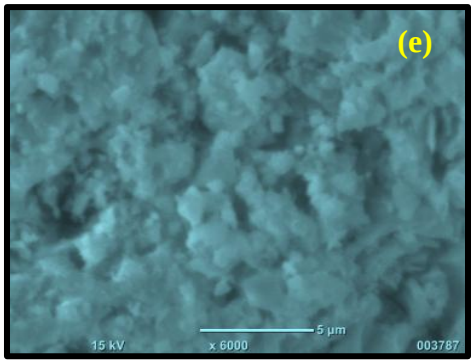


Fig 4. The SEM micrographs of $SnO_2$: CuO nanostructured thin films.

**Optical Properties and Energy Band Gap from UV-Vis Analysis**

From the UV-Vis analysis as illustrated in Fig 5, it was clearly seen that, the maximum absorption peak for $SnO_2$ with CuO ( 0.02 g) was observed between 325 nm and 375 nm. The absorbance slightly increased at that region 325 nm and 380 nm for CuO ( 0.04 g ) doping. The absorption peaks were spread out between 330 nm and 380 nm for CuO ( 0.06 g ). $SnO_2$ with CuO ( 0.08 g ) doping was observed to be the high absorbance at 335 nm. And $SnO_2$ with CuO ( 0.1 g ) doping was revealed that the absorbance was broader and higher at 340 nm and 370 nm. Tauc's relation was used to calculate band gap energies and variation of $(\alpha h\upsilon)^2$ versus $h\upsilon$ were shown in Fig 6(a, b, c, d and e). The obtained band gap energies of $SnO_2$:CuO thin films were listed in Table 4.

Table 4. The band gap energies of $SnO_2$:CuO thin films.

| No | CuO (g) | Band gap energy (eV) |
|---|---|---|
| 1 | 0.02 | 3.35 |
| 2 | 0.04 | 3.28 |
| 3 | 0.06 | 3.22 |
| 4 | 0.08 | 3.29 |
| 5 | 0.1 | 3.32 |

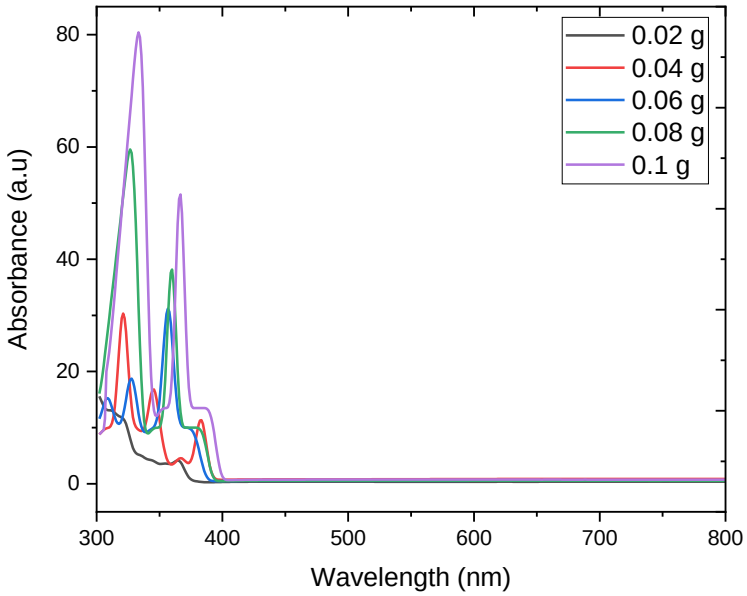


Fig 5. The UV-Vis spectra of $SnO_2$:CuO nanostructured thin films.

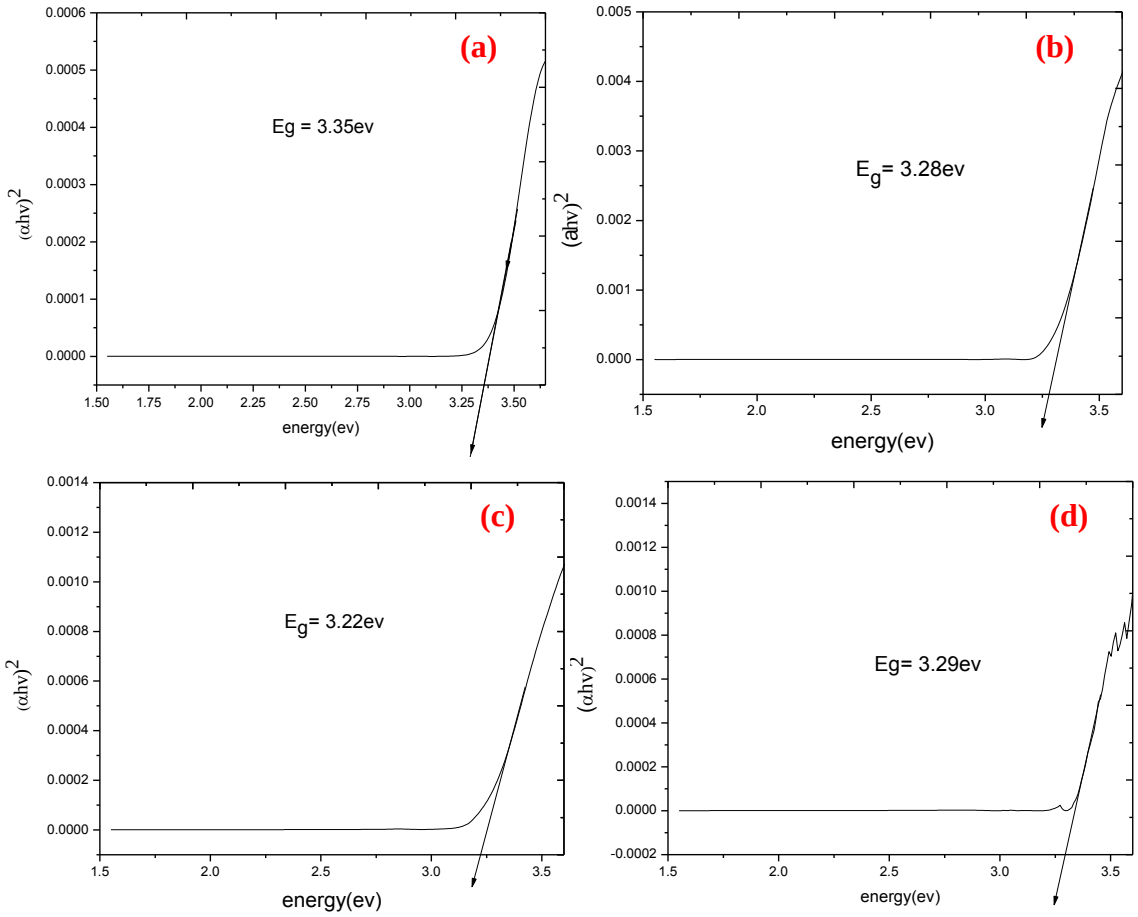

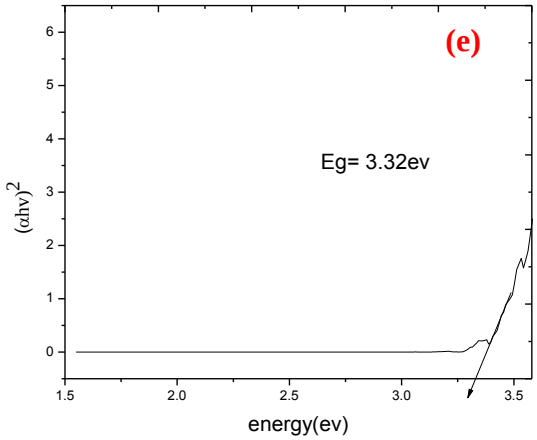


Fig 6. The energy band gap of $SnO_2$:CuO nanostructured thin films.

## Conclusion

$SnO_2$:CuO nanostructured thin films were successfully fabricated by sol-gel method. According to the XRD analysis the crystal structure of CuO:$SnO_2$ nanostructured thin films were shown tetragonal crystal structure. The average crystallite sizes of $SnO_2$:CuO (0.02, 0.04, 0.06, 0.08 and 0.1g) nanostructured thin films were 52.035 nm, 26.927 nm, 37.757 nm, 30.874 nm and 17.517 nm. The surface morphological properties of the fabricated thin films were characterized with SEM and it was revealed that the grain size distribution depended on the amount of CuO doping. UV-Vis Spectroscopy analysis showed that the optical absorbance were maximum in the wavelength between 325 nm and 380 nm. The band gap energies of fabricated thin films were observed to be in the range of 3.35 eV to 3.22 eV. It was also noted that the values of energy band gap were approached to narrow range which could be converted to p-type semiconductor from to n-type semiconductor. From this research work it was concluded that the obtained $SnO_2$:CuO nanostrucured thin films were quite suitable for photovoltaic applications such as solar cells and gas sensing applications.

### Acknowledgement

This research work was totally implemented in Materials Research Lab, Department of Physics, University of Mandalay.

### References

A. Sinopoli *et al*., Solar Energy. **86** (2012) 1563.

I. S. Hwang, J. K. Choi., S. J.Kim, Dong K. Y., Kwon J. H., Ju B. K., *et al*., Sensor & Actuator B - Chem .**142** (2009) 105-109.

M. Atif *et al*., Materials. **8** (2015) 355.
M. EL. Nahass *et al*., Trans. NonFerrous Met. Soc. **22** (2012) 3003.
S. Galioglu *et al*., Microporous and Mesoporous materials. **196** (2014) 136.

S. Rani, S. C. Roy, N. Karar, M. C. Bhatnagar, *et al*., Solid State Commun.**141** (2007) 214-218.

W. Junbo, Y. Minge, L. C. Yingmin, Licheng, *et al*., Non-Cryst Solids, **351** (2015) 228-232.